Porous Cu-rich@Cu$_3$Pt alloy catalyst with a low Pt loading for enhanced electrocatalytic reactions

Jin-Yeon Lee, Sang-Beom Han, Da-Hee Kwak, Min-Cheol Kim, Seul Lee, Jin-Young Park, In-Ae Choi, Hyun-Suk Park, Kyung-Won Park[*]

Department of Chemical Engineering, Soongsil University, Seoul, 156-743, Republic of Korea

ABSTRACT

The core-shell nanostructures are used to improve the specific activity of catalysts in electrooxidation reactions. We report a porous Cu-rich@Cu$_3$Pt core-shell using a seeding method. In this method, a hetero-nucleation process is carried out in the presence of cubic Cu$_2$O seeds. Cu-rich@Cu$_3$Pt core-shell is used as an electrocatalyst in electrooxidation reactions. According to the data obtained using transmission electron microscopy (TEM), energy dispersive X-ray analysis (EDX), and X-ray diffraction (XRD), Cu-rich@Cu$_3$Pt has a porous nanostructure and dominant {111} facets. It consists of a well-defined core-shell structure in which a Cu-rich phase is the core and Cu$_3$Pt alloy is the shell. The porous Cu-rich@Cu$_3$Pt exhibits an excellent electrocatalytic performance in methanol oxidation reaction (MOR) and oxygen reduction reaction (ORR).

© 2016 Elsevier B.V. All rights reserved.

1. Introduction

Direct methanol fuel cells (DMFCs) have received intensive interests as a promising candidate of clean energy source for powering portable electronic devices and electric vehicles [1–3]. At the anode of DMFCs, methanol oxidation reaction (MOR) is a complex process involving the exchange of six electrons and formation of intermediates such as CHO or CO [4–6]. In this reaction, active catalytic sites are required for adsorption and oxidation of methanol. Furthermore, active catalytic sites are also required for the oxidation and desorption of adsorbed intermediates of MOR [7]. Currently, Pt-based alloy or core-shell nanoparticles have been comprehensively studied and utilized as anodic electrocatalysts in MOR, which takes place in DMFCs [8–12]. Moreover, proton exchange membrane fuel cells (PEMFCs) have also been considered as a promising alternative power source because they have a fast startup procedure, high energy efficiency, low operating temperature, and environmental friendliness [13,14]. In PEMFCs, Pt is the most effective catalyst that facilitates oxygen reduction reaction (ORR) [15–19]. However, owing to the high cost and scarcity of Pt, the application of ORR has been hindered. As a result, we have not been able to achieve widespread commercialization of fuel cell technologies [20,21]. In these systems, Pt and Pt-based nanostructure materials are efficiently used in acidic media as anode and cathode [22,23].

Pt-based bimetallic nanoparticles (NPs), such as core-shell and its alloys, have well-controlled morphology and structure that exhibits optimized electrochemical properties in catalytic reactions [24–26]. Moreover, the core-shell structured NPs are also capable of generating enhanced electrocatalytic properties, which are driven by electronic interactions between the Pt shell and the second metal core as well as the Pt shell nanostructures with different geometries, such as islands, monolayer, and intermixing phase [27,28]. Furthermore, in order to improve specific mass activity in electrocatalytic reactions, the core-shell nanostructures are placed on the exposed surface structures of platinum atoms, while the thin layer of shell structures is in the core-shell NPs [29–31]. Especially, the core-shell cathode catalysts having transition metals such as Fe, Co, Ni, and Cu as a core have intensively been studied. Mukerjee et al. reported fundamental aspects of Cu dissolution and contamination in CuSO$_4$-doped 0.1 N solutions of HClO$_4$ and H$_2$SO$_4$ under both inert and oxygenated conditions [32]. Strasser and co-workers proposed Pt-Cu dealloyed core-shell catalysts for an improved ORR activity, which result in a shift of the electronic band structure of Pt [33]. In addition, Jia et al. showed that the atomic distribution of Pt-based bimetallic NPs under operating conditions

---

was strongly dependent on the initial atomic ratio [34].

In particular, dendritic and flower-like Pt-based nanostructures have shown an enhanced electrocatalytic activity and stability in electrochemical power sources, because they have porous structures with particular facets that favor electrocatalytic reactions [35–37]. In this study, we synthesized porous core-shell NPs (denoted as porous Cu-rich@Cu$_3$Pt), which were used as electrocatalysts through a seeding method in which hetero-nucleation process was carried out in the presence of Cu$_2$O nanocube seeds. The crystal structure, elemental composition, morphology, and chemical states of porous Cu-rich@Cu$_3$Pt were characterized by XRD analysis, field-emission transmission electron microscopy (FE-TEM), EDX spectroscopy, and X-ray photoelectron spectroscopy (XPS). The electrochemical properties of the as-prepared electrocatalysts in MOR and ORR were measured and compared using a potentiostat.

2. Experimental

2.1. Synthesis of porous Cu-rich@Cu$_3$Pt NPs

0.01 M copper(II) chloride dihydrate (CuCl$_2$·2H$_2$O, 99.0%, Aldrich) and 2 M sodium hydroxide (NaOH, 98.0%, Samchun) were mixed in de-ionized (DI) water at 50 °C. Then, 0.6 M L-ascorbic acid (C$_6$H$_8$O$_6$, 99.0%, Aldrich) was added in the solution and stirred for 3 h. After completing the reaction, the final precipitate was obtained as a seed for porous Cu-rich@Cu$_3$Pt. The precipitate (0.04 g) as a seed and 0.01 g hydrogen hexahydroxyplatinate(IV) (H$_2$Pt(OH)$_6$, 99.9%, Aldrich) were mixed in 450 mL of DI-water at 50 °C with continuous stirring. Then, 0.6 M L-ascorbic acid was added in the mixed solution containing the seed in the absence of surfactant. The solution of Cu-rich@Cu$_3$Pt was kept at 50 °C for 3 h until the Pt salts were completely reduced on the core. The resulting colloidal solution, which was black in color, was cooled down to 25 °C. To prepare Cu-rich@Cu$_3$Pt nanoparticles (40 wt%) supported on carbon black (Vulcan XC-72R), carbon power was mixed and stirred in the colloid solution. The pH of the mixture solution was adjusted to 2, and then, washed it with ethanol and de-ionized water. Thereafter, the products were dried in an oven at 50 °C.
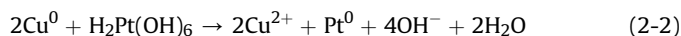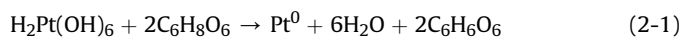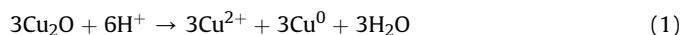
2.2. Structural and chemical analysis

The morphology and size of the catalysts were characterized by FE-TEM using a Tecnai G^2 F30 system, which was operated at 300 kV. The TEM samples were prepared by placing drops of catalyst suspension, which was dispersed in ethanol on a carbon-coated nickel grid. The EDX analysis of the catalysts was performed on a FE-TEM. To determine the structure of the catalysts, XRD analysis was carried out using a Bruker X-ray diffractometer (D2 PHASER, Bruker AXS) with a Cu K$_\alpha$ ($\lambda = 0.15418$ nm) source and a Ni filter. The source was operated at 30 kV and 10 mA. The 2θ angular scan was performed from 20° to 80° at a scan rate of 0.02° min^{-1}. XPS (Thermo Scientific, K-Alpha) analysis was carried out using an Al K$_\alpha$ X-ray source of 1486.6 eV in a chamber pressure below 1×10^{-8} Torr and 200 W beam power. The high resolution spectra were obtained using a pass energy of 46.95 eV. The step size and time per step were chosen to be 0.025 eV and 100 ms, respectively. Both the ends of the baseline were set sufficiently far apart, to avoid distortion in the shape of the spectra, including the tails. A small variation in the range of the baseline did not affect the relative number of fitted species (less than 1%). The C 1s electron binding energy was referenced at 284.6 eV, and a Gaussian-Lorentzian production function was applied using a nonlinear least-squares curve-fitting program.

2.3. Electrochemical analysis

The electrochemical properties of the as-prepared electrocatalysts for MOR and ORR were measured in a three-electrode cell at 25 °C using a potentiostat (Eco Chemie, AUTOLAB). The electrocatalyst inks were prepared by mixing the electrocatalyst powder, DI water, 2-propanol solution (99.5%, Aldrich), and 5 wt% Nafion® solution (Aldrich). The glassy carbon working electrode was coated with electrocatalyst inks and dried at 50 °C in an oven. The Pt loading amounts of porous Cu-rich@Cu$_3$Pt catalysts were 5.2 and 10.0 μg cm^{-2} in MOR and ORR, respectively. And loading amount of comm-Pt catalysts were 40.0 μg cm^{-2} in MOR and ORR, respectively. In addition, Pt wire and Ag/AgCl (in saturated 3 M KCl) were used as counter and reference electrodes, respectively. To compare the electrochemical properties and MOR activity of the samples, cyclic voltammograms (CVs) of the electrocatalysts were obtained in Ar-saturated 0.1 M HClO$_4$ and 0.1 M HClO$_4$ + 2.0 M CH$_3$OH with a scan rate of 50 mV s^{-1} at 25 °C. To evaluate the electrocatalytic stability of MOR, the electrocatalysts were kept at 0.45 V for 7200 s in 0.1 M HClO$_4$ + 2.0 M CH$_3$OH and CVs were then obtained in 0.1 M HClO$_4$ + 2.0 M CH$_3$OH after the stability test. The current-potential curves of ORR were obtained in O$_2$-saturated 0.1 M HClO$_4$ solution by sweeping the potential from 0.8 to 0.0 V with a rotation speed of 1600 rpm at a scan rate of 5 mV s^{-1}. The stability test of ORR was carried out by applying a linear potential sweep for 2000 cycles between 0.4 and 0.9 V with a rate of 50 mV s^{-1} in O$_2$-saturated 0.1 M HClO$_4$ solution at 25 °C. The oxygen reduction current-potential curves after the stability test of the electrocatalysts were obtained by sweeping the potential from 0.8 to 0.0 V at a scan rate of 5 mV s^{-1} and a rotating disk speed of 1600 rpm.

3. Results and discussion

Fig. 1(a)-(c) show TEM images of Cu$_2$O, which was synthesized through a chemical reaction. The as-prepared Cu$_2$O exhibited a cubic shape (denoted as cubic-Cu$_2$O), which had an average size of ~111.5 nm (Fig. 2(a)). The cubic-Cu$_2$O exhibited a d-spacing of 0.216 nm, which corresponded to (200) plane of the reference Cu$_2$O (JCPDS No. 77–0199) (Fig. 1(c)). Fig. 1(d) and (e) show TEM images of the as-synthesized NPs having a porous spherical shape with the agglomeration of many small NPs and an average particle size of ~41.9 nm (Fig. 2(b)). Interestingly, the shell region of porous Cu-rich@Cu$_3$Pt NP exhibited {111} facets, having a d-spacing of 0.213 nm. The Cu$_3$Pt alloy phase exhibited a face-centered-cubic (fcc) crystal structure (Fig. 1(f)). On the other hand, in the core region of the Cu-rich alloy phase, Pt represents the {111} facets with a d-spacing of 0.211 nm. To identify the elemental distribution of NPs, a linear profile and an elemental mapping image of the core-shell NPs were obtained as shown in Fig. 1(g) and (h), respectively. The as-prepared NPs contain dominant Cu (red) in the core region, while Pt (green) mixed with Cu in the shell region. As shown in Fig. 1(i), the core-shell NPs were synthesized by a seeding method in which Pt was grown through heterogeneous nucleation. The cubic-Cu$_2$O NPs as seeds in this process were reduced to Cu-rich phase as a core material (Eq. (1) of disproportionation process) and the Cu$_3$Pt alloy shell was subsequently formed on the Cu-rich core (Eqs. (2-1) and (2-2)) [38,39].

$$3Cu_2O + 6H^+ \rightarrow 3Cu^{2+} + 3Cu^0 + 3H_2O \tag{1}$$

$$H_2Pt(OH)_6 + 2C_6H_8O_6 \rightarrow Pt^0 + 6H_2O + 2C_6H_6O_6 \tag{2-1}$$

$$2Cu^0 + H_2Pt(OH)_6 \rightarrow 2Cu^{2+} + Pt^0 + 4OH^- + 2H_2O \tag{2-2}$$

Furthermore, as confirmed by EDX, the NPs are elemental